INTERNATIONAL JOURNAL OF AGRICULTURE & BIOLOGY
ISSN Print: 1560–8530; ISSN Online: 1814–9596
17–006/2017/19–4–735–745
DOI: 10.17957/IJAB/15.0348
http://www.fspublishers.org

Full Length Article

Overexpression of *2-Cys Prx* Increased Salt Tolerance of Photosystem Ⅱ in Tobacco

Hui-hui Zhang[1†], Nan Xu[2,3†], Xin Li[1], Wei-wei Jin[3], Qi Tian[3], Si-yu Gu[1*] and Guang-yu Sun[3*]
[1]*College of Resources and Environment, Northeast Agricultural University, Harbin, Heilongjiang, P.R. China*
[2]*Natural Resources and Ecology Institute, Heilongjiang Sciences Academy, Harbin Heilongjiang, P.R. China*
[3]*College of Life Science, Northeast Forest University, Harbin Heilongjiang, 150040, P.R. China*
[*]For correspondence: sungy@vip.sina.com; gsyneau@163.com
[†]Equal contributors

Abstract

To explore the plant active oxygen scavenging and photosynthesis function of 2-Cys Prx, a newly discovered member of the antioxidant protease family, the tobacco *2-Cys Prx* gene was cloned into the plant expression vector prok II. This vector, which is controlled by the constitutive strong promoter CaMV35S, was introduced into tobacco by *Agrobacteria*-mediated transformation. The 816-bp open reading frame of tobacco *2-Cys Prx* encodes 271 amino acids and showed high homology with *2-Cys Prx* genes from *Solanum lycopersicum*, *Vitis vinifera*, and *Populus trichocarpa*, indicating *2-Cys Prx* gene is highly conserved. The active oxygen metabolism and chlorophyll fluorescence response to salt stress were also studied. Under salt stress, superoxide dismutase (SOD) activity in tobacco leaves increased, while ascorbate peroxidase (APX) activity decreased. Additionally, the donor- and acceptor-side function of photosystem II (PSII) were affected by salt stress to different degrees, with the latter significantly more affected than the former. The H_2O_2 and malondialdehyde content of *2-Cys Prx*- overexpression tobacco leaves under salt stress were all significantly lower than those of wild-type (CK) leaves. The PSII maximum photochemical efficiency (F_v/F_m) and the performance index on absorption basis (PI_{ABS}) of *2-Cys Prx*- overexpression leaves were significantly lower than those of CK leaves under salt stress. Various relative fluorescence intensities of the *2-Cys Prx*-overexpression plants exhibited significantly lower increases in amplitude than those of CK plants. Thus, *2-Cys Prx* increased the salt tolerance of PSII function and lowered the PSII light inhibition effect in plants under salt stress, suggesting that *2-Cys Prx* gene overexpression can alleviate H_2O_2 buildup and lower the peroxide levels of cytomembrane lipids under salt stress. Thus, *2-Cys Prx* gene overexpression can protect oxygen-evolving complex function at the donor side of PSII under salt stress and improve electron transfer at the acceptor side of PSII.

Keywords: Peroxiredoxin; Transgenic plants; Tobacco; Reactive oxygen species; Photosynthetic characteristics

Introduction

When a plant is under stress, an excess of electrons may accumulate in its photosynthesis electron transport chain. If not promptly cleared, these electrons can attack monovalent oxygen molecules and form superoxide anions in the thylakoid membranes of chloroplasts (Reddy *et al.*, 2004). Superoxide dismutase (SOD) within chloroplast stroma and the lumen of higher plants can remove H_2O_2 formed by superoxide anions (Hayakawa *et al.*, 1984, 1985); therefore, the main reactive oxygen species (ROS) in chloroplasts are H_2O_2, rather than superoxide anions. H_2O_2 can damage DNA, proteins, carbohydrates and lipids in cells and can also induce programmed cell death (Liang *et al.*, 2003). In addition, H_2O_2 can generate highly active and extremely destructive hydroxyl free radicals through the Haber–Weiss reaction catalyzed by iron (Sun *et al.*, 2005). These hydroxyl radicals can damage the compositional subunits of the oxygen-evolving complex (OEC) and hamper its turnover (Henmi *et al.*, 2004). Most ROS in chloroplasts under stress are produced by an excess of electrons in the photosynthetic electron transport chain, while ROS, in turn, hinder the normal transmission of photosynthetic electrons through their attack on the electron transporters and consequently inhibit normal photosynthesis in plants (Jiao *et al.*, 2002; Farooq *et al.*, 2009, 2015). Thus, removing ROS in chloroplasts, especially H_2O_2, is essential for the protection of normal photosynthesis from stress. However, plants do not have H_2O_2 scavenger catalase in their chloroplasts. In higher plant chloroplasts, H_2O_2 clearance is completed by ascorbate peroxidase (APX) (Asada, 2000; Aran *et al.*, 2009). There are typically 10–30 mmol·L^{-1} of APX in the chloroplasts of higher plants (Nakano and Asada, 1987), but APX is very sensitive to excessive ROS under extreme stress (Dietz *et al.*, 2002). Under high ROS level conditions, APX activity is significantly

To cite this paper: Zhang, H.H., N. Xu, X. Li, W.W. Jin, Q. Tian, S.Y. Gu and G.Y. Sun, 2017. Overexpression of *2-Cys Prx* increased salt tolerance of photosystem Ⅱ in tobacco. *Int. J. Agric. Biol.*, 19: 735–745

reduced (Dietz, 2003; Santos and Rey, 2006).

Peroxiredoxin (Prx) is a protein (without metal combining subunits) that removes ROS in organisms through the oxidation of the conserved cysteine residue (-Cys) (Pena-Ahumada *et al.,* 2006). Prx exists in a variety of organisms (Horling *et al.,* 2001; Jang *et al.,* 2006). In eukaryotes, Prx plays a leading role in the removal of ROSc (Winterbourn, 2008; Cox *et al.,* 2009). In higher plants, four members of the Prx family have been identified: 1-Cys Prx, 2-Cys Prx, Prx II, and Prx Q. The *2-Cys Prx* protein is found in chloroplasts though it is encoded by a nuclear gene (Baier and Dietz, 1996; Baier *et al.,* 2000). It is specifically located in the thylakoid membrane of the chloroplast, and its sequence is highly conserved (Bhatt and Tripathi, 2011; Baier and Dietz, 1996). In *Arabidopsis thaliana*, two subtypes of *2-Cys Prx* have been identified: *2-Cys Prx* A and *2-Cys Prx* B (Brehelin *et al.,* 2003). Under low APX activity conditions in plant chloroplasts, *2-Cys Prx* plays an important role in the oxidation–reduction process, specifically in the clearing of H_2O_2 (Rouhier and Jacquot, 2002; König *et al.,* 2003). Wood *et al.* (2003) found that *2-Cys Prx* can regulate H_2O_2 concentration by transient reversible oxidative inactivation, that is, *2-Cys Prx* can remove H_2O_2 selectively (Wood *et al.,* 2003). In addition, *2-Cys Prx* can also exist in the form of complexes with high molecular weights, in which the proteins are connect as two dimers by a Cys83–Cys83 disulfide bond or form a decamer consisting of five identical dimmers. They participate in the physiological and pathological processes in plants as molecular chaperones (Rhee *et al.,* 2007; Lim *et al.,* 2008), and the activity of the decamer is often higher than the activity of the dimer (Lee *et al.,* 2007; Kang *et al.,* 2012).

Under stress conditions, ROS, especially H_2O_2 in chloroplasts, can not only cause the accumulation of peroxidation product malondialdehyde (MDA) in chloroplast membranes (Sun *et al.,* 2009), but also attack the His residues in D1 protein, thus inhibiting electron transport on the photosynthetic electron transport chain, reducing photosystem II (PSII) reaction center activity and inhibiting photosynthesis (Wei *et al.,* 2004). Therefore, if *2-Cys Prx* can clear ROS in chloroplasts, then *2-Cys Prx* may play a role in the protection of PSII electron transport in plants under stress? If may play a role, which parts in PS II? What kind of role play? Contreras *et al.* (2010) found that *2-Cys Prx* expression can be induced by abiotic stress, and enhanced *2-Cys Prx* expression can effectively improve resistance to abiotic stress (Broin *et al.,* 2002; König *et al.,* 2002). The component of PSII within the chloroplast and thylakoid membrane are the most sensitive parts of plants to environmental changes; many studies have shown that stress affects PSII function (Jiang *et al.,* 2002; Lu and Vonshak, 2002). However, the mechanism of the salt stress effect of *2-Cys Prx* on PSII photochemical activity is not clear. To test the photoprotection effect of *2-Cys Prx* in plants under stress, *2-Cys Prx* was cloned from tobacco, linked to the prokII expression vector, and transducted into tobacco (*Nicotiana tabacum*) using *Agrobacteria* to obtain tobacco plants that overexpress 2-Cys Prx. These plants were used as experimental materials and compared to wild-type (CK) control plants. The differences in ROS metabolism and photosynthetic functions of PSII between the *2-Cys Prx*-overexpression tobacco leaves and CK control under stress conditions were studied, and the role of *2-Cys Prx* in the photoprotection mechanism in plants was explored.

Materials and Methods

Experimental Details and Treatments

Experimental material: Tobacco variety 'Longjiang 911' was provided by the Tobacco Institute in Mudanjiang City, Heilongjiang Province, China. Plant expression vector prokII was provided by the State Key Laboratory for Forest Genetics and Breeding at State Key Laboratory of Tree Genetics and Breeding, Northeast Forestry University, Heilongjiang, China. *Agrobacteria* strain LBA 4404 and competent *E. coli* Trans1-T1 cells were purchased from TransGen Biotech (Beijing, China). A reverse transcription kit was purchased from Invitrogen (Carlsbad, CA, USA). DL2000 DNA Marker and DL15000 DNA Marker were purchased from TaKaRa (Shiga, Japan). Taq polymerase, Pfu polymerase, and restriction enzymes were purchased from Promega (Madison, WI, US). The pJET cloning vector was purchased from HaiGene (Manilla, Philippines). T4 DNA ligase was purchased from GeneCopoeia (Rockville, MD, USA). Primer synthesis and sequencing were conducted by Beijing Genomics Institute (BGI).

Cloning 2-Cys Prx

The full-length sequence of tobacco *2-Cys Prx* obtained from the GenBank database (AJ309009.2) was used for primer design. Table 1 shows the primer sequences of *2-Cys Prx*- S and *2-Cys Prx*- A used in this study. Tender leaves from the top of wild-type tobacco plants were sampled for total RNA extraction using the CTAB method (Chang *et al.,* 1993), and extracted RNA was subjected to reverse transcription into cDNA after DNA digestion. The *2-Cys Prx*- specific primers were used for PCR amplification with the synthesized cDNA as template. PCR products were separated by 1.0% agarose gel electrophoresis, and the DNA fragments were recovered, purified, and linked to the pJET cloning vector. The recombinant vector was then transformed into competent *E. coli* Trans1-T1 cells, and successfully transformed colonies were selected by ampicillin resistance. Single clones were picked, and *2-Cys Prx* expression was verified by PCR of the bacteria colonies. The amplified fragments were sequenced by BGI.

Vector Construction

After the *2-Cys Prx* positive clone was confirmed by

sequencing, primers containing the sequences of *Xba*I and *Kpn*I digestion sites *Xba*I-*2-Cys Prx*- S and *Kpn*I -*2-Cys Prx*- A (Table 1) were used for the PCR reaction. A pJET-*2-Cys Prx* plasmid was used as the template to obtain the PCR product of the *2-Cys Prx* gene containing the digestion sites. Then the PCR product and the prok Ⅱ vector were double digested by *Xba*I and *Kpn*I, and the digested DNA fragments were recovered after gel electrophoresis using gel extraction kits (Omega, Norcross, GA, USA). The *2-Cys Prx* and vector sequences were ligated, heat activated, and transformed to obtain a prokII-*2-Cys Prx* plasmid. After verification by sequencing, the plasmid was introduced into *Agrobacteria* by electroporation to obtain an *Agrobacteria* strain containing the *2-Cys Prx* gene.

Agrobacteria-mediated Transformation and Generation of Transgenic Tobacco Plantlets

Agrobacteria were cultured to their logarithmic phase (OD600 between 0.4 and 0.5), and then they were used to infect tobacco leaves. The tobacco leaves were cultured on MS solid medium for 3 days, and then they were transferred to selection MS solid medium containing 0.05 $mg \cdot L^{-1}$ NAA, 0.5 $mg \cdot L^{-1}$ 6-BA, 50 $mg \cdot L^{-1}$ kanamycin, and 300 $mg \cdot L^{-1}$ cephalosporin. When the adventitious buds grew to about 1.0 cm long, they were transferred to MS rooting medium containing 50 $mg \cdot L^{-1}$ kanamycin and 300 $mg \cdot L^{-1}$ cephalosporin.

Identification of Transgenic Tobacco

Tobacco leaf DNA extracted by the CTAB method (Porebski *et al.,* 1997) was used as PCR template, and CaMV35S promoter-specific primers were used for the PCR reaction (CaMV35S-S and CaMV35S-A primer sequences are shown in Table 1). The PCR thermal cycling conditions were as follows: 30 s at 94°C for denaturation, 30 s at 62°C for annealing, and 60 s at 72°C for extension, repeated for a total of 35 cycles. PCR products were separated by 1.0% agarose gel electrophoresis. The target fragment was approximately 800 bp in length.

Treatments

The *2-Cys Prx*- positive plants were removed from the culture media. The residual culture media was washed off from the root surface, and the plants were place into half-strength Hoagland solution for liquid culture for 20 days with 200 $\mu mol \cdot m^{-2} \cdot s^{-1}$ of light and temperatures of 25–30°C with a 12/12 h (light/dark) photoperiod. Non-transgenic tobacco (i.e. CK) was used as control. After culturing for 20 days, the transgenic and CK tobacco seedlings with relatively consistent growth were transferred into half-strength Hoagland solution containing NaCl concentrations of 0, 50, 100 and 200 $mmol \cdot L^{-1}$ for salt stress treatments. Five plants were used in each treatment. The physiological and photosynthetic functions of the tobacco seedlings leaves were tested after 48 h of salt treatment.

Table 1: Sequences of PCR primers

Primer name	Sequence (5'-3')
2-Cys Prx-S	5'-ATGGCTTGCTGCTTCTTCTA-3'
2-Cys Prx-A	5'-TCATATGGATGCAAAGTATTCTTG-3'
*Xba*I-2-Cys Prx-S	5'-GCTCTAGACAATGGCTTGCTGC-3'
*Kpn*I-2-Cys Prx-A	5'-CGGGGTACCGGTCTCCAGCCTTCCTA-3'
CaMV35S-S	5'-AGATTAGCCTTTTCAATTTCAGAAAG-3'
CaMV35S-A	5'-CGTGTTCTCTCCAAATGAAATGAAC-3'

The Measured Items and Methods

SOD activity was determined using the nitro blue tetrazolium (NBT) method. The amount of enzyme required to photochemically reduce 50% of NBT in 1 mL of reaction solution in a 1-h unit of time (1 h) was considered one enzymatic activity unit (U), and the enzymatic activity units in each g of fresh samples were described as $U \cdot g^{-1}$ (Li and Chen, 1998). APX activity was determined using the method by Shen Wenbiao (Shen *et al.,* 1996). The enzyme activity units (again, U) were defined as the amount of enzyme used to catalyze the oxidation of 1 μmol of ascorbic acid in 1 min, and the enzyme activity unit in each g of fresh samples was described as $U \cdot g^{-1}$. H_2O_2 content was determined using the method by Lin Zifang (Lin *et al.,* 1988). MDA content was determined using the method by Wang (Wang *et al.,* 2003).

Chlorophyll fluorescence parameter determination was assessed using the second to last fully expanded leaf of the plant in each treatment, which was selected for dark adaptation lasting 0.5 h. A mini modulated handheld chlorophyll fluorometer (FluorPen FP 100 max; Photon Systems Instruments, Drasov, Czech Republic) was used to measure the OJIP curves of leaves under different treatments. Each measurement was repeated three times. The OJIP curve was assessed under 3000 $\mu mol \cdot m^{-2} \cdot s^{-1}$ pulse red light, and the recording of the fluorescence signals started at 10 μs after exposure and stopped at 1 s after exposure, and 10^5 data points per second were recorded. The average values of the fluorescence intensity of the five OJIP curves under different treatments at each time point were calculated, and OJIP curves using the average values were plotted. The time points of 0.01, 0.15, 0.3, 2.0, 30 and 1000 ms after exposure on the OJIP curve were defined as the O, L, K, J, I, and P points, respectively. The O–P, O–J, and O–K curves were standardized, and were expressed as $V_{O–P}$, $V_{O–J}$ and $V_{O–K}$, respectively. The O–P curve was standardized as $V_{O–P}=(F_t-F_o)/(F_M-F_o)$. The O–J curve was standardized as $V_{O–J}=(F_t-F_o)/(F_J-F_o)$. The O–K curve was standardized as $V_{O–K}=(F_t-F_o)/(F_K-F_o)$. In these formulas, F_t represents the fluorescence intensity at each time point. The relative fluorescence intensities V_J and V_I at points J and I on the $V_{O–P}$ curve, the relative fluorescence intensity of V_K at point K on the $V_{O–J}$ curve and the relative fluorescence intensity V_L at point L on the $V_{O–K}$ curve were each calculated. The differences in the values of the $V_{O–P}$, $V_{O–J}$, and $V_{O–K}$ curves of tobacco leaves treated at different salt

concentrations were calculated respectively and the differences were expressed as ΔV_{O-P}, ΔV_{O-J} and ΔV_{O-K}, respectively. The JIP-test method by Strasser and Srivastava (1995) was used to analyze the OJIP curve to obtain the chlorophyll fluorescence parameters, which are the PSII maximum photochemical efficiency (F_v/F_m), and performance index on absorption basis (PI_{ABS}).

Statistical Analysis

The statistical analysis of enzyme activities and chlorophyll fluorescence parameters was performed using Excel (Microsoft, Redmond, WA, USA) and SPSS (version 22.0; IBM Corp., Armonk, NY, USA). A one-way analysis of variance and subsequent least significant difference procedures were used to compare the differences between different treatments.

Results

Cloning and Sequence Analysis of *2-Cys Prx*

In this study shows that the full length open reading frame of the tobacco *2-Cys Prx* gene was 816 bp, encoding 271 amino acids (Fig. 1–2). A comparison of the gene sequence of tobacco *2-Cys Prx* with other gene sequences in the NCBI database, showed amino acid sequence homology as high as 90% between the tobacco *2-Cys Prx* gene sequence and the *2-Cys Prx* gene in tomato (*Solanum lycopersicum*) and the homologies with grape (*Vitis vinifera*) and *Populus trichocarpa* were as high as 81%.

Acquisition and Verification of *2-Cys Prx* Transgenic Plant

The CaMV35S-prokII-*2-Cys Prx* expression vector was obtained by insertion of *2-Cys Prx* into the CaMV35S-prokⅡ vector (Fig. 3). The expression vector was electroporated into *Agrobacteria*-4404 after sequence verification and then introduced into tobacco by *Agrobacteria*-mediated transformation. After 2 weeks of differentiation and selection, the resistant buds started to appear at the edges of the tobacco leaves. When the plantlets grew to 1.0 cm in length, they were transferred to rooting medium. A total of 42 plantlets were obtained.

The transgenic tobacco plants were texted by PCR using CaMV35S strong promoter-specific primers, and a total of 32 plants showed the expected 800-bp PCR fragment. The non-transgenic control did not show the PCR fragment (partial results are shown in Fig. 4). The results showed that the *2-Cys Prx* overexpression vector had been successfully transformed into tobacco plants.

Effect of Salt Stress on SOD and APX Activities in *2-Cys Prx*-overexpression Tobacco

This is shows that as salt concentration increased the SOD activity of tobacco seedling leaves increased,

```
   1 atggcttgctctgcttcttctacagcacttctttcttccaaccca
  M A C S A S S T A L L S S N P
 46 aaagcagcttccatttccccccaaatcctcctttcaagctcccatt
  K A A S I S P K S S F Q A P I
 91 tctcaatgtttatctgtaccttcctctttcaatgggctccgtaat
  S Q C L S V P S S F N G L R N
136 tgcaagccttttgtttctcgtgtagcccgttccctctctactcgc
  C K P F V S R V A R S L S T R
181 gttgctcaatcccaacgccgtcgtttcgttgttcgtgcctctagt
  V A Q S Q R R R F V V R A S S
226 gaacttccacttgttggaaatcaagcgccagactttgaggctgaa
  E L P L V G N Q A P D F E A E
271 gctgtttttgatcaagaattcatcaaggttaaactatctgagtac
  A V F D Q E F I K V K L S E Y
316 attgggaagaagtatgtcattctctttttctacccactagacttt
  I G K K Y V I L F F Y P L D F
361 acatttgtttgcccaacagagatcactgctttcagtgaccgttat
  T F V C P T E I T A F S D R Y
406 ggagaatttgaaaagttgaacacagaaatattgggtgtttccgta
    G E F E K L N T E I L G V S V
451 gacagtgtgttctcccaccttgcctgggtccaaaccgaaagaaag
      D S V F S H L A W V Q T E R K
496 tctggtgggctaggtgatttgaactatccattaatttctgacgtg
      S G G L G D L N Y P L I S D V
541 accaagtcaatttcaaaatcatacaatgtactgatccccgatcag
      T K S I S K S Y N V L I P D Q
586 ggaattgcattgagaggacttttcatcattgacaaggaaggagtt
      G I A L R G L F I I D K E G V
631 attcagcattcaaccattaacaatcttggaattggtcggagtgtt
      I Q H S T I N N L G I G R S V
676 gatgaaacattgagaactcttcaggcattgcaatacgttcaggat
      D E T L R T L Q A L Q Y V Q D
721 aacccggatgaagtgtgcccagctggatggaagcctggggagaaa
      N P D E V C P A G W K P G E K
766 tccatgaagcctgaccccaagggtagcaaagaatactttgcatcc
      S M K P D P K G S K E Y F A S
811 atatga 816
    I *
```

Fig. 1: *Nicotiana tabacum 2-Cys Prx* gene sequence and amino acid sequence alignment

while APX activity decreased (Fig. 5). At salt on centration of 0 and 50 mmol·L^{-1}, the SOD activities in the leaves of *2-Cys Prx*-overexpression and CK tobacco plants were nearly the same, but when the salt concentration reached 100 mmol·L^{-1}, the SOD activities in the leaves of the two types of plants significantly increased. When salt concentrations were 100 and 200 mmol·L^{-1}, the SOD activities in the leaves of *2-Cys Prx*- overexpression tobacco plants were 9.26% ($P > 0.05$) and 5.84% ($P > 0.05$) lower than those of CK leaves, respectively, but the difference between these decreases were not statistically significant. The APX activities in the two types of tobacco leaves were

Fig. 2: Alignment of *Nicotiana tabacum 2-Cys Prx* (Nt 2-Cys Prx) protein sequence with the protein sequences of *Solanum lycopersicum 2-Cys Prx* (Sl 2-Cys Prx), *Vitis vinifera 2-Cys Prx* (Vv 2-Cys Prx), and *Populus trichocarpa 2-Cys Prx* (Pt 2-Cys Prx)

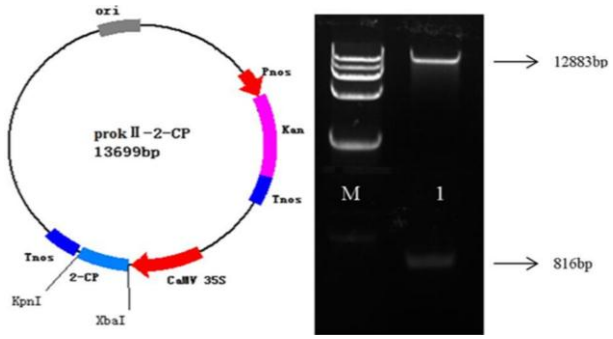

Fig. 3: The construction map of 35S:: prok Ⅱ::2- Cys Prx and the test of the expression vector of prok Ⅱ::2-Cys Prx
Note: M: DNA maker DL15000; 1: The test product of the expression vector of prok Ⅱ::2-Cys Prx

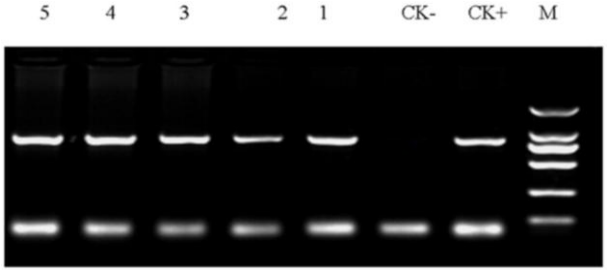

Fig. 4: PCR identification of transgenic tobacco plants
The lanes contained the following samples: M, DL2000 DNA marker; CK+, 35S::prok Ⅱ::*2-Cys Prx* plasmid; CK-, wild-type tobacco; 1-5, 2-Cys Prx-overexpression tobacco line

significantly reduced when the salt concentration was increased to 100 mmol·L^{-1}, but the differences in APX activities between the *2-Cys Prx*-overexpression and CK tobacco leaves under different salt concentrations were not significant.

Effect of Salt Stress on H_2O_2 and MDA Contents in *2-Cys Prx*- overexpression Tobacco

As salt concentrations increased, the H_2O_2 and MDA contents of both control and experimental plants

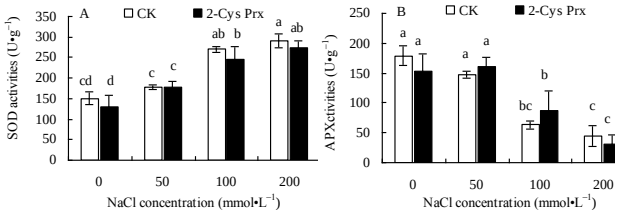

Fig. 5: Effect of salt stress on the superoxide dismutase (A) and ascorbate peroxidase activities (B) in leaves of CK and 2-*Cys Prx*-overexpression tobacco plants. Data in the figures are means ± S.E., Bar graphs depict mean ± SE, values followed by different small letters mean significant difference (p<0.05)
than those of the CK leaves, respectively. The differences were all statistically significant

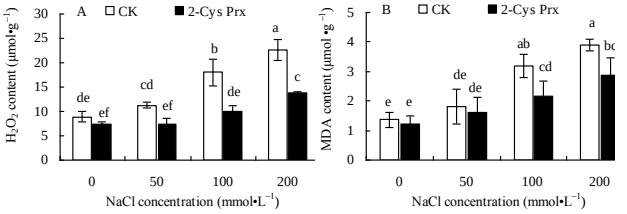

Fig. 6: Effect of salt stress on the H_2O_2 (A) and malondialdehyde MDA (B) contents in leaves of CK and 2-Cys-Prx overexpression tobacco plants. Bar graphs depict mean ± SE, values followed by different small letters mean significant difference (p<0.05)

increased (Fig. 6). When the salt concentration was 0 mmol·L^{-1}, H_2O_2 and MDA contents of the *2-Cys Prx* overexpression leaves were slightly lower than those of CK leaves, but the differences were not significant. When the salt concentration increased to 50 mmol·L^{-1}, H_2O_2 and MDA contents in CK leaves increased 26.97% (P < 0.05) and 63.77% (P < 0.05), respectively, but the H_2O_2 and MDA contents of the *2-Cys Prx*-overexpression leaves showed no significant changes. As the salt concentrations increased further, the H_2O_2 and MDA contents of the two types of tobacco leaves increased significantly, but when salt concentrations were 100 and 200 mmol·L^{-1}, the H_2O_2 contents of the *2-Cys Prx* overexpression leaves were 45.00% (P < 0.05) and 38.94% (P < 0.05) lower than those of the CK leaves, respectively, and the MDA contents were 32.50% (P < 0.05) and 26.15% (P < 0.05) lower.

Effect of Salt Stress on the OJIP curve in *2-Cys Prx*-overexpression Tobacco Leaves

Under different salt stress conditions, the relative fluorescence intensities at point O of the OJIP curve of CK tobacco leaves were all significantly increased compared with those plants not in a salt stress condition (Fig. 7). The relative fluorescence intensities at point P under salt concentrations of 100 and 200 mmol·L^{-1} were significantly

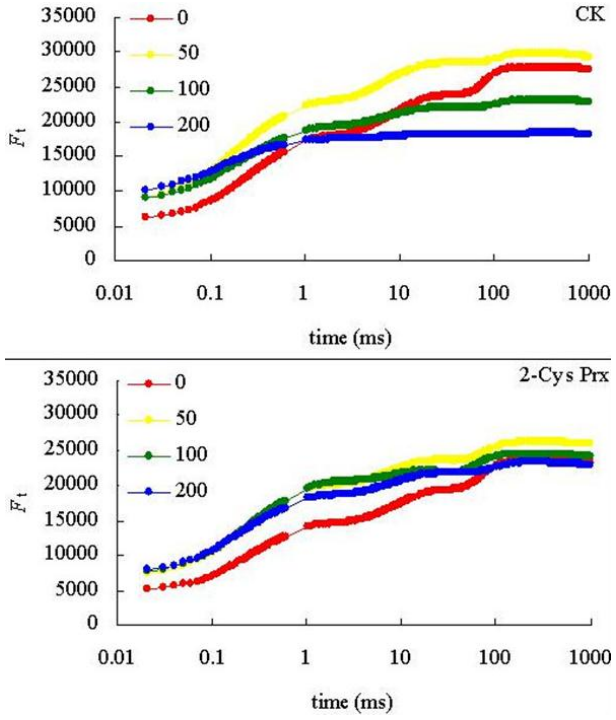

Fig. 7: Effect of salt stress on the chlorophyll *a* fluorescence transient (i.e., the OJIP curve) in CK and 2-Cys Prx-overexpression tobaccos

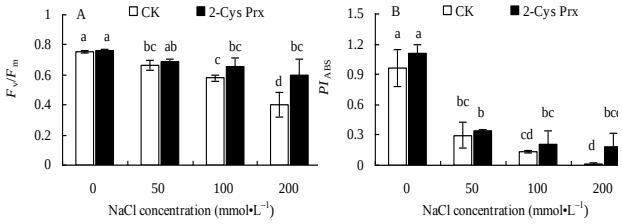

Fig. 8: Effect of salt stress on F_v/F_m (A) and PI_{ABS} (B) in leaves of CK and 2-Cys Prx-overexpression tobacco plants. Bar graphs depict mean ± SE, values followed by different small letters mean significant difference (p<0.05)

decreased, and at 200 mmol·L^{-1} salt stress, the extent of the decrease in the relative fluorescence intensity at point P was significantly larger than those under the 100 mmol·L^{-1} salt stress treatment, that is, with increasing salt concentrations, the OJIP curves of the tobacco leaves were flatter. Under salt stress conditions, the relative fluorescence intensities in the leaves of *2-Cys Prx*- overexpression tobacco at point O on the OJIP curve were also significantly increased, but there were no significant differences among salt concentration treatments, and the relative fluorescence intensities at point P showed no significant changes compared to those under no salt stress, but the relative fluorescence intensities at points J and I were significantly increased.

Effect of Salt Stress on F_v/F_m and PI_{ABS} in *2-Cys Prx*-overexpression Tobacco

Increased salt concentration significantly decreased both F_v/F_m and PI_{ABS} in both experimental and CK tobacco seedlings, but the extent of decrease in the *2-Cys Prx*-overexpression tobacco was significantly smaller than that in CK tobacco (Fig. 8). As salt concentrations increased, the differences between the two types of tobaccos increased gradually. When salt concentrations were 0 and 50 mmol·L^{-1}, there were no significant differences in F_v/F_m values between the experimental and control plants, but when the salt concentrations were 100 and 200 mmol·L^{-1}, the F_v/F_m values in the leaves of the *2-Cys Prx*-overexpression plants were 12.88% (P > 0.05) and 49.83% (P < 0.05) higher than those in the leaves of CK plants, respectively. In addition, when the salt concentration was increased to 200 mmol·L^{-1}, the PI_{ABS} values in the leaves of *2-Cys Prx*- overexpression plants were 2.64 times those in the leaves of CK plants.

Effect of Salt Stress on the Standardized O-P Curve of *2-Cys Prx*- overexpression Plants

According to the standardized OJIP curves under different salt concentrations, the relative variable fluorescence at points J and I (V_J and V_I, respectively) in leaves of tobacco plants at salt concentrations of 50, 100 and 200 mmol·L^{-1} were all significantly increased compared to those at a salt concentration of 0 mmol·L^{-1} (Fig. 9). Moreover, the variation amplitude of V_J was significantly larger than that of V_I. The V_J and V_I values in the leaves of CK tobacco plants increased with salt concentration. However, although the V_J and V_I values in the leaves of *2-Cys Prx*-overexpressing tobacco were significantly increased at salt concentrations of 50, 100 and 200 mmol·L^{-1} compared to the V_J and V_I values at the 0 mmol·L^{-1} salt concentration, the differences among the three different salt treatments were relatively small.

At a salt concentration of 200 mmol·L^{-1}, the value of V_J in *2-Cys Prx*- overexpression tobacco was 18.54% (P<0.05) lower than that of CK plants, but when the salt concentrations were 0, 50 and 100 mmol·L^{-1}, the V_J values showed no significant differences between the two types of tobacco (Fig. 10). The V_I values of *2-Cys Prx*-overexpression tobacco at salt concentrations of 0, 50, 100, and 200 mmol·L^{-1} were 4.72% (P < 0.05), 7.47% (P< 0.05), 8.93% (P < 0.05), and 8.64% (P < 0.05) lower than the V_I values of CK plants, respectively, and the differences were all statistically significant.

Effect of Salt Stress on the Standardized O-J curve in *2-Cys Prx*- overexpression Tobacco

The relative variable fluorescence at 0.3 ms of point K (V_K) on the standardized O-J curves significantly differed among different salt concentration treatments (Fig. 11).

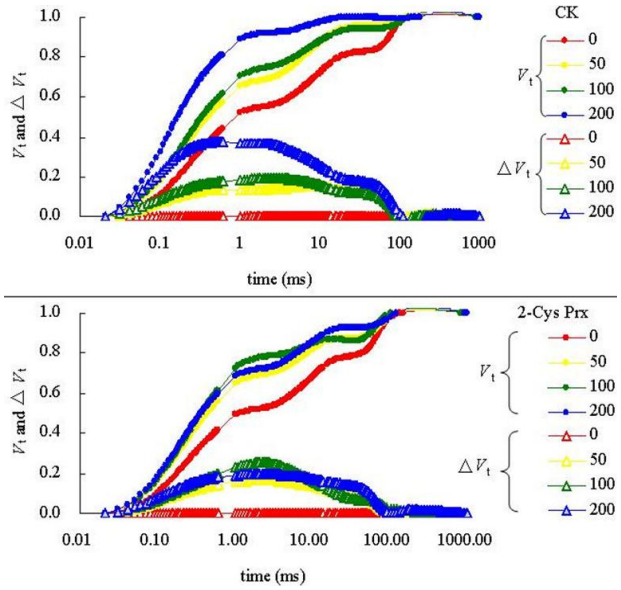

Fig. 9: Effect of salt stress on chlorophyll *a* fluorescence transients (i.e., OJIP curves). The OJIP curves were normalized between F_o to F_P using the equation $V_t = (F_t - F_o)/(F_P - F_o)$ and then subtracting the kinetics estimated from CK plants (at a NaCl concentration of 0 mmol·L^{-1}) from the kinetics of different salt stress treatments (i.e., $\triangle V_{O–P} = V_{O–P\ (salt)} - V_{O–P\ (CK)}$) in CK and 2-Cys Prx-overexpression tobacco

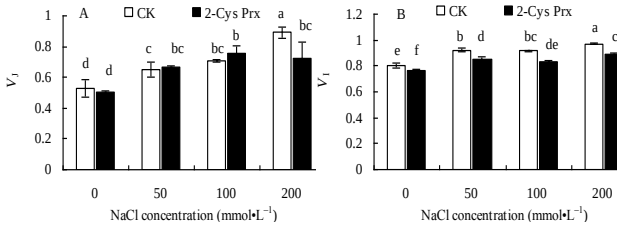

Fig. 10: Effect of salt stress on V_J (A) and V_I (B) in CK and 2-Cys Prx-overexpression tobacco. Bar graphs depict mean ± SE, values followed by different small letters mean significant difference (p<0.05)

With the salt concentration increases, the V_K values in tobacco leaves showed obvious increasing trends, but the extent of the V_K increase in *2-Cys Prx*-overexpression tobacco was significantly lower than that in CK tobacco. Quantitative analysis showed (Fig. 12) that, at salt concentrations of 50, 100, and 200 mmol·L^{-1}, the V_K values of the *2-Cys Prx*-overexpression tobacco were 5.62% (P<0.05), 8.96% (P<0.05), and 13.71% (P < 0.05) lower than those of the CK leaves, respectively, and the differences were all statistically significant. With the increase in salt concentrations, the differences between the two types of tobaccos were more obvious.

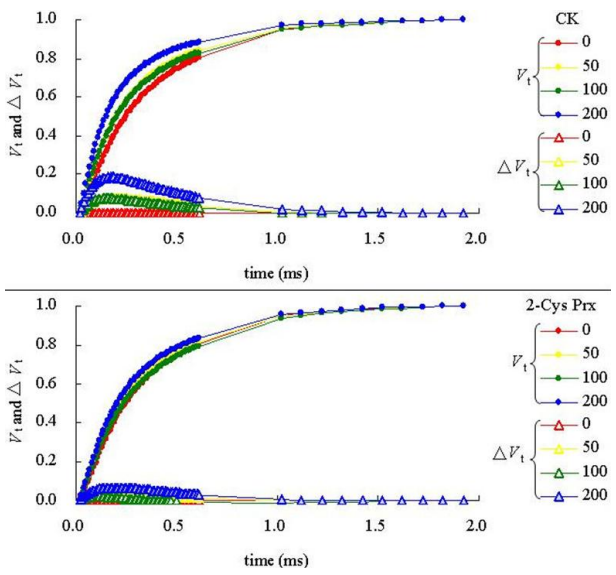

Fig. 11: Effect of salt stress on chlorophyll *a* fluorescence transients (at O–J) were normalized between F_o to F_J, as determined by using the equation $V_t = (F_t - F_o)/(F_J - F_o)$ and then subtracting the kinetics estimated from CK plants (at a NaCl concentration of 0 mmol·L^{-1}) from the kinetics under different salt concentration treatments (i.e., $\triangle V_{O–J} = V_{O–J\ (salt)} - V_{O–J\ (CK)}$) in CK and 2-Cys Prx-overexpression tobacco

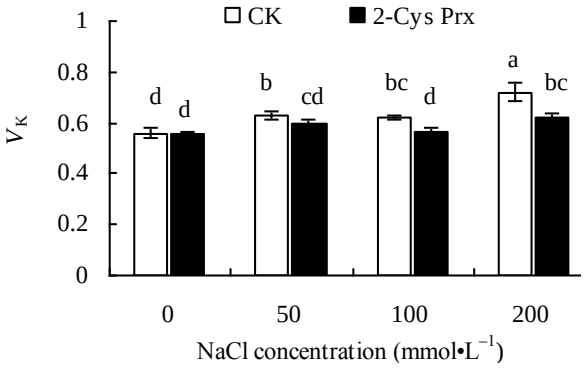

Fig. 12: Effect of salt stress on V_K in CK and 2-Cys Prx-overexpression tobacco. Bar graphs depict mean ± SE, values followed by different small letters mean significant difference (p<0.05)

Effect of Salt Stress on the Standardized O–K curve in *2-Cys Prx*- overexpression Tobacco

The relative variable fluorescence of point L at 0.15ms (V_L) on the standardized O–K curve significantly differed under different salt concentration treatments (Fig. 13). As salt concentration increased, the V_L values significantly increased, but the extent of the increase in *2-Cys Prx*-overexpression tobacco were significantly smaller than those of CK tobacco. Quantitative analysis showed that

(Fig. 14), at salt concentrations of 50, 100 and 200 mmol·L^{-1}, the V_L values in *2-Cys Prx* overexpression tobacco were 2.74% (P > 0.05), 5.77% (P > 0.05) and 10.86% (P < 0.05) lower than those of CK tobacco, respectively. However, the differences between the experimental and control tobacco plants were statistically significant only at a salt concentration of 200 mmol·L^{-1}.

Discussion

In this study, the tobacco *2-Cys Prx* gene was cloned and found to have amino acid sequence homologies as high as 90% with sequences from other species (Fig. 2). This indicates that *2-Cys Prx* is highly conserved. Plant expression vector 35S-prok II-2Cys Prx containing the 35S promoter was then constructed and transducted into tobacco. Molecular verification and physiological testing was then conducted on the 2Cys Prx-overexpression tobacco.

Kim *et al.* (2013) transferred the *2-Cys Prx* gene from rice (*Oryza sativa*) into *Saccharomyces cerevisiae* and found that the heterologous expression of *2-Cys Prx* in *S. cerevisiae* increased the oxidation–reduction balance in *S. cerevisiae* 40°C, indicating that *2-Cys Prx* effectively regulates the reactive oxygen balance in organisms. H_2O_2 in plant cells is the intermediate product in the process of water splitting and oxygen liberation. When the function of the water splitting complex is suppressed, H_2O_2 is generated. When the function of the water splitting complex is normal, most H_2O_2 molecules are produced by the dismutation effect of SOD (Zhu *et al.*, 2007). In chloroplasts, H_2O_2 produces hydroxyl radical (OH) through the Haber–Weiss reaction, which causes peroxidation in the lipid of the chloroplast membrane, thereby increasing levels of the peroxidation product MDA in the chloroplast membrane (Jiang *et al.*, 1994). Therefore, the removal of H_2O_2 from chloroplasts is an important part of relieving oxidation stress in plants. Jiang (2011) indicated that enhanced *2-Cys Prx* expression could significantly improve the germination rate and seedling antioxidant level of transgenic tobacco under salt stress. Additionally, overexpression of the peroxide protein (PreQ) gene in corn (*Zea mays*) could increase plant resistance to fungi and enhance anti-oxidation ability (Kiba *et al*., 2005). In our study, as salt concentration increased, SOD activities in the cells also increased, and H_2O_2 produced by superoxide anion dismutation increased, but at the same time, APX activity, which can remove H_2O_2, decreased significantly. The excess of H_2O_2 increased MDA content in tobacco leaf membranes, and the cells suffered serious oxidative stress (Fig. 5; Fig. 6). However, when there were no significant differences in the SOD and APX activities between the CK and *2-Cys Prx*- overexpression tobaccos, the H_2O_2 and MDA contents of *2-Cys Prx*- overexpression tobacco were significantly lower than those of CK tobacco. Especially under the high salt stress condition that induced large decreases in APX activity, the differences in H_2O_2 and

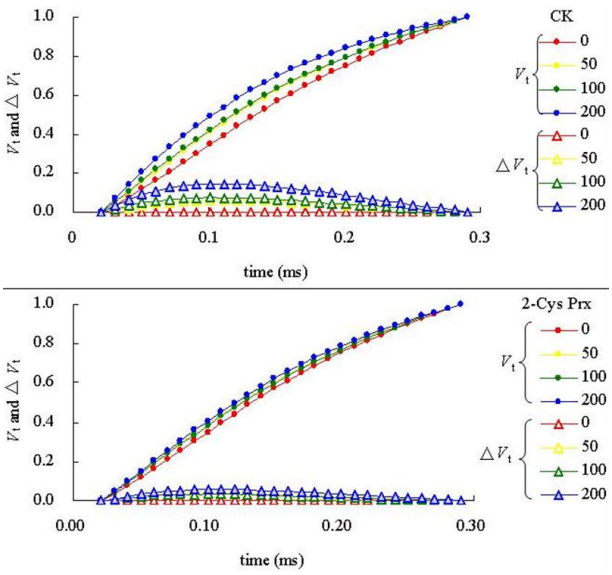

Fig. 13: Effect of salt stress on chlorophyll *a* fluorescence transients (O–K), which were normalized between F_o and F_K using the equation V_t = (F_t - F_o)/(F_K - F_o) and subsequently subtracting the kinetics estimated from CK plants (at a NaCl concentration of 0 mmol·L^{-1}) from the kinetics at different concentration salt stress ($\triangle V_{O-K}$ = $V_{O-K(salt)}$ - $V_{O-K(CK)}$) in CK and 2-Cys Prx-overexpression tobacco

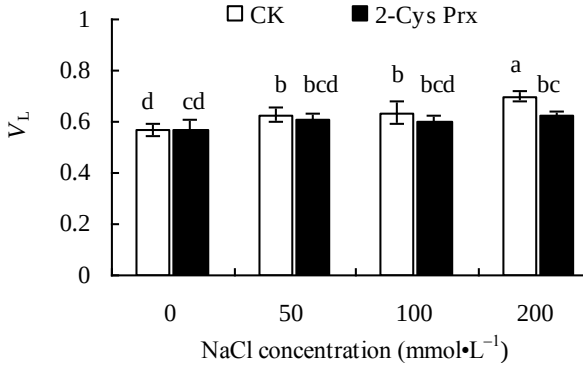

Fig. 14: Effect of salt stress on V_L in CK and 2-Cys Prx-overexpression tobacco. Bar graphs depict mean ± SE, values followed by different small letters mean significant difference (p<0.05)

MDA contents were more pronounced, indicating that under severe stress, overexpression of *2-Cys Prx* can effectively alleviate H_2O_2 and reduce membrane lipid peroxidation levels.

The reduced photosynthesis of plants under salt stress is related to salt-induced ROS imbalance in plant cells (Yang *et al.*, 2007; Assaha *et al.*, 2015). The activities of plant ribulose-1,5- diphosphate carboxylase (i.e., RuBisCo) and the regeneration rate of ribulose-1,5-diphosphate (i.e., RuBP) are decreased under salt stress (Vu

et al., 1987), and the dark reaction process of photosynthesis is also suppressed, which reduces the ability to assimilate ATP and NADPH. This creates feedback inhibition on the electron transfer in the photosynthetic electron transport chain, resulting in the accumulation of excess electrons and generation of ROS (Zhang *et al.,* 2012a). Studies have found that *2-Cys Prx* mainly occurs on the thylakoid membrane (König *et al.,* 2002, 2003). Through western blot analysis of the plant thylakoid membrane, Meenakumari *et al*. (2009) found that *2-Cys Prx* and PSII are closely associated (Meenakumari *et al.,* 2009). Baier and Dietz (1999) found that inhibition of *2-Cys Prx* expression significantly reduced photosynthesis in *Arabidopsis thaliana* (Baier and Dietz, 1996; Nelson and Shem, 2004). Therefore, if *2-Cys Prx* scavenges ROS, then overexpression of *2-Cys Prx* in tobacco could effectively protect PSII reaction center function under salt stress. To investigate this model, this study used the chlorophyll fluorescence analysis technique to examine changes in photosynthetic apparatus function in tobacco leaves under salt stress. As salt concentrations increased, the OJIP curves in both experimental and control tobacco leaves showed obvious changes. The values of F_v/F_m and PI_{ABS} decreased in young leaves from both types of plants, but the extent of the decrease in *2-Cys Prx*- overexpression tobacco plants was significantly smaller than that in the CK tobacco plants, that is, the overexpression of *2-Cys Prx* significantly alleviated the extent of photoinhibition of PSII under salt stress. To further examine the mechanism for the differences in the PSII reaction center activities, OJIP curves of the tobacco leaves under different salt concentration treatments were also examined. As the chlorophyll fluorescence increased from the initial fluorescence up to the maximum fluorescence (that is, from O point to P point), there were two distinctly notable points, J and I. Point J reflects the accumulation of Q_A^-, and point I reflects the accumulation of Q_B^-. In other words, the increase in the relative variable fluorescence at point J (i.e., V_J) indicates a blockage of the electron transfer from the primary electron acceptor Q_A to the secondary electron acceptors Q_B at the electron transfer acceptor side (Xia *et al.,* 2004; Chen *et al.,* 2005); meanwhile, the increase in the relative variable fluorescence at point I (i.e., V_I) indicates a blockage of electron transfer from Q_B to PQ (Ohad and Hirschberg, 1992; Kiba *et al.,* 2005). In this study, as salt concentrations increased, the values of V_J and V_I significantly increased, indicating that salt stress inhibits electron transfer at the PSII acceptor side in both types of tobacco plants. However, the values of V_J and V_I in *2-Cys Prx*- overexpression tobacco across all salt concentrations were lower than those of CK tobacco. In other words, under salt stress, the electron transfer rate at the PSII acceptor side in *2-Cys Prx* overexpression tobacco were significantly higher than those of CK tobacco. Nishiyama *et al.* (2011) demonstrated that ROS can inhibit PSII repair by inhibiting D1 protein synthesis, resulting in a decrease in PSII activity and, thus, more excess excitation energy is produced, thereby inducing more ROS and creating a harmful positive feedback loop (Nishiyama *et al.,* 2011). The secondary electron acceptor Q_B in the photosynthetic electron transport chain is mainly attached to D1 proteins and functions in electronic transmission (Jiang, 2011; Zhang *et al.,* 2013b); therefore, the relative increase of PSII acceptor side electron transfer in the *2-Cys Prx*-overexpression tobacco may be caused by the effective protection of D1 protein under stress, but this finding requires further verification.

To analyze the effect of the oxygen-evolving complex (OEC) on the PSII donor side in different salt treatments and to exclude the influence of the PSII acceptor side, the O–J portion of the OJIP curve was standardized. An increase in the relative variable fluorescence at point K, corresponding to 0.3 ms (V_K) on the standardized O–J curve, was related to the inhibition of PSII electron donor side activity, especially the activity of the OEC (Li *et al.,* 2009). The values of V_K showed obvious increasing trends in the tobacco leaves, but the increase in V_K values was significantly lower than the increase in V_J and V_I values. In other words, the salt stress damage to the acceptor side was significantly higher than the salt stress damage to the donor side, in agreement with previous findings (Zhang *et al.,* 2013a). The increase in V_K values in the *2-Cys Prx*-overexpression tobacco was significantly lower than that in CK tobacco, and the V_K values in the *2-Cys Prx*-overexpression tobacco was significantly lower than those in CK tobacco at various salt concentrations, indicating that salt stress can lower OEC activity. Bertamini and Nedunchezhian found that OEC activity was reduced by the stress induced degradation of the 33-kDa hydrolyzing protein complex or the failed efficient connection between OEC and PSII (Bertamini and Nedunchezhian, 2000). Alternatively, this may be caused by the degradation of the OEC core component Psa0 protein. However, under salt stress, especially under high salt concentrations, the damage to the OEC in *2-Cys Prx*- overexpression tobacco was significantly less severe than the damage to the CK tobacco. Under stress, the OEC damage resulted in incomplete water splitting and H_2O_2 production. This may be one of the causes of the increase of H_2O_2 in tobacco leaves under salt stress (Fig. 6). However, the H_2O_2 content in *2-Cys Prx*- overexpression tobacco was significantly lower than that in CK tobacco. In addition to effectively removing H_2O_2 in cells, *2-Cys Prx* overexpression can also effectively reduce damage to the OEC under salt stress. This is one of the main reasons that *2-Cys Prx*-overexpression tobacco showed relatively less oxidation damage under salt stress. ROS generated under stress in plant cells can directly lead to the destruction of the thylakoid membrane structure. Photosynthetic electron transporters are attached to the thylakoid membrane; damage to the thylakoid membrane thus further reduces electron transfer capacity. Therefore, stability of the thylakoid membrane structures ensures the activity of the

optical system. The increase in the relative variable fluorescence at point L (i.e., V_L) on the standardized O–K curve is a reliable indicator of thylakoid membrane damage (Zhang *et al.*, 2012b; Ye *et al.*, 2013). As salt concentration increases, the V_L values of tobacco leaves significantly increased, but the extent of the increase in V_L values in *2-Cys Prx*- overexpression tobacco was significantly lower than those of CK tobacco. This indicates that under salt stress, *2-Cys Prx* overexpression can increase the stability of the thylakoid membrane structures, and these results are consistent with its effect on electron transfer at both the donor and acceptor side of PSII.

Conclusion

Under salt stress-induced low-APX activity conditions, overexpression of *2-Cys Prx* can effectively remove excess H_2O_2 from tobacco cells. This not only reduces the degree of cell membrane peroxidation, but also alleviates the degree of inhibition of the PSII reaction center under salt stress.

Acknowledgments

This research was supported by The National Natural Science Fund (31500323; 31400429). Harbin science and Technology Innovation Talents(2013RFXXJ063).

References

Aran, M., D.S. Ferrero, E. Pagano and R.A. Wolosiuk, 2009. Typical 2-Cys peroxiredoxins-modulation by covalent transformations and non covalent interactions. *FEBS. J*., 276: 2478–2483

Asada, K., 2000. The water–water cycle as alternative photon and electron sinks. *Phil. Trans. R. Soc. Lond. B.*, 1402: 1419–1430

Assaha, D.V.M., L. Liu, A.M.M. Mekawy, A. Ueda, T. Nagaoka and H. Saneoka, 2015. Effect of salt stress on Na accumulation, antioxidant enzyme activities and activity of cell wall peroxidase of huckleberry (*Solanum scabrum*) and eggplant (*Solanum melongena*). *Int. J. Agric. Biol*., 17: 1149–1156

Baier, M. and K.J. Dietz, 1996. Primary structure and expression of plant homologues of animal and fungal thioredoxin-dependent peroxide reductases and bacterial alkyl hydroper-oxide reductases. *Plant Mol. Biol*., 31: 553–564

Baier, M. and K.J. Dietz, 1999. Protective function of chloroplast 2-cysteine peroxiredoxin in photosynthesis. Evidence from transgenic Arabidopsis. *Plant Physiol*., 119: 1407–1414

Baier, M., G. Noctor, C.H. Foyer and K.J. Dietz, 2000. Antisense suppression of 2-cysteine peroxiredoxin in arabidopsis specifically enhances the activities and expression of enzymes associated with ascorbate metabolism but not glutathione metabolism. *Plant Physiol*., 124: 823–832

Bertamini, M. and N. Nedunchezhian, 2003. Photoinhibition of photosynthesis in mature and young leaves of grapevine (*Vitis vinifera* L.). *Plant Sci.*, 4: 635–644

Bhatt, I. and B.N. Tripathi, 2011. Plant peroxiredoxins: Catalytic mechanisms, functional significance and future perspectives. *Biotechnol. Adv*., 29: 850–859

Brehelin, C., E.H. Meyer, J.P.D. Souris and Y. Meyer, 2003. Resemblance and dissemblance of Arabidopsis type II peroxiredoxins: similar sequences for divergent gene expression, protein localization, and activity. *Plant Physiol*., 132: 2045–2057

Broin, M., S. Cuine, F. Eymery and P. Rey, 2002. The plastidic 2-cysteine peroxiredoxin is a target for a thioredoxin involved in the protection of the photosynthetic apparatus against oxidative damage. *Plant Cell*, 14: 1417–1432

Chang, S., J. Puryear and J. Cairney, 1993. A simple and efficient method for isolating RNA from pine trees. *Plant Mol. Biol. Rep.*., 11: 113–116

Chen, S.G., X.B. Dai, S. Qiang and Y. Tang, 2005. Effect of a nonhost-selective toxin from *Alternariata alternata* on chloroplast-electron transfer activity in *Eupatorium adenophorum*. *Plant Pathol*., 54: 671–677

Contreras, L., A. Moenne., F. Gaillard., P. Potind and J.A. Correaa, 2010. Proteomic analysis and identification of copper stress-regulated proteins in the marine alga *Scytosiphon gracilis* (Phaeophyceae). *Aquat. Toxicol*., 96: 85–89

Cox, A.G., C.C. Winterbourn and M.B. Hampton, 2009. Mitochondrial peroxiredoxin involvement in antioxidant defence and redox signalling. *Biochem. J*., 425: 313–325

Dietz, K.J., 2003. Plant peroxiredoxins. *Ann. Rev. Plant Biol*., 54: 93–107

Dietz, K.J., F. Horling, J. Konig and M. Baier, 2002. The function of the chloroplast 2-cysteine peroxiredoxin in peroxide detoxification and its regulation. *J. Exp. Bot*., 53: 1321–1329

Farooq, M., A. Wahid, N. Kobayashi, D. Fujita and S.M.A. Basra, 2009. Plant drought stress: effects, mechanisms and management. *Agron. Sustain. Dev*., 29: 185–212.

Farooq, M., M. Hussain, A. Wakeel and K.H.M. Siddique, 2015. Salt stress in maize: effects, resistance mechanisms and management. A review. *Agron. Sustain. Dev*., 35:461–481

Hayakawa, T., S. Kanematsu and K. Asada, 1984. Occurrence of Cu, Zn-superoxide dismutase in the intrathylakoid space of Spinach chloroplasts. *Plant Cell Physiol*., 25: 883–889

Hayakawa, T., S. Kanematsu and K. Asada, 1985. Purification and characterization of thylakoid-bound Mn-superoxide dismutase in Spinach chloroplasts. *Planta*, 166: 111–116

Henmi, T., M. Miyao and Y. Yamamoto, 2004. Release and reactive-oxygen-mediated damage of the oxygen-evolving complex subunits of PSII during photoinhibition. *Plant Cell Physiol*., 45: 243–250

Horling, F., M. Baier and K.J. Dietz, 2001. Redox-regulation of the expression of the peroxide-detoxifying chloroplast 2-Cys peroxiredoxin in the liverwort Riccia fluitans. *Planta*, 214: 304–313

Jang, H.H., S.Y. Kim, S.K. Park, H.S. Jeon, Y.M. Lee, J.H. Jung, S.Y. Lee, H.B. Chae, Y.J. Jung, K.O. Lee, C.O. Lim, W.S. Chung, J.D. Bahk, D.J. Yun, M.J. Cho and S.Y. Lee, 2006. Phosphorylation and concomitant structural changes in human 2-Cys peroxiredoxin isotype I differentially regulate its peroxidase and molecular chaperone function. *FEBS. Lett*., 580: 351–355

Jiang, B., 2011. *Salt Tolerance Analysis of a 2-Cys Prx Gene from Tamarix Androssowii*. Mater Dissertation of Northeast Forestry University, Harbin, China

Jiang, C.D., H.Y. Gao and Q. Zou, 2002. Characteristics of photosynthetic apparatus in Mn-starved leaves. *Photosynthetica*, 40: 209–213

Jiang, M.Y., W.Y. Yang, J. Xu and Q.Y. Cheng, 1994. Active oxygen damage effect of chlorophyll degradation in rice seedlings under osmitic stress. *Acta. Bot. Sin*., 6: 289–295

Jiao, D.M., X. Li, X.Q. Huang and B.H. Ji, 2002. The Relationship among photoinhibition, photooxidation and early aging at later developmental stages in different high yield varieties. *Sci. Agric. Sin*., 35: 487–492

Kang, R.X., Z.X. Liu, Y. Liu, Y.H. Li and Y. Jiang, 2012. The regulation of Prx1 in cell signal transduction. *Prog. Mod. Biomed*., 12: 2186–2190

Kiba, A., M. Nishihara, N. Tsukatani, T. Nakatsuka, Y. Kato and S.A. Yamamura, 2005. peroxiredoxin Q homolog form gentians is involved in both resistance fungal disease and oxidative stress. *Plant Cell Physiol*., 46: 1007–1015

Kim, I.S., Y.S. Kim and H.S. Yoon, 2013. Expression of salt-induced 2-Cys peroxiredoxin from *Oryza sativa* increases stress tolerance and fermentation capacity in genetically engineered yeast *Saccharomyces cerevisiae*. *Appl. Microbiol. Biotechnol*., 97: 3519–3533

König, J., K. Lotte, R. Plessow, A. Brockhinke, M. Baier and K.J. Dietz, 2003. Reaction mechanism of plant 2-Cys peroxiredoxin. Role of the Cterminus and the quaternary structure. *J. Biol. Chem*., 278: 24409–24420

König, J., M. Baier, F. Horling, U. Kahmann, G. Harris, P. Schürmann and K.J. Dietz, 2002. The plant-specific function of 2-Cys peroxiredoxin-mediated detoxification of peroxides in the redox-hierarchy of photosynthetic electron flux. *Proc. Natl. Acad. Sci*., 99: 5738–5743

Lee, W., K.S. Choi, J. Riddell, I. Clement, D. Ghosh, J.H Park and Y.M. Park, 2007. Human peroxiredoxin 1 and 2 are not duplicate proteins: the unique presence of CYS83 in Prx1 underscores the structural and functional differences between Prx1 and Prx2. *J. Biol. Chem*., 282: 22011–22022

Li, H.S. and C.L. Chen, 1998. *The Experiment Principle and Technology of Plant Physiology*. Wuhan: Huazhong Agricultural University press

Li, P.M., L.L. Cheng, H.Y. Gao and T. Peng, 2009. Heterogeneous behavior of PSII in soybean (*Glycine max*) leaves with identical PSII photochemistry efficiency under different high temperature treatments. *J. Plant Physiol*., 166: 1607–1615

Liang, Y.C., F. Hu, M.C. Yang and J.H. Yu, 2003. Antioxidative defenses and water deficitinduced oxidative damage in rice (*Oryza sativa* L.)growing on non-flooded paddy soils with ground mulching. *Plant Soil*, 257: 407–416

Lim, J.C., H.I. Chio and Y.S. Park, 2008. Irreversible oxidation of the active-site cysteine of peroxiredoxin to cysteine sulfonic acid for enhanced molecular chaperone activity. *J. Biol. Chem*., 283: 28873–28880

Lin, Z.F., S.S. Li, G.Z. Lin and J.Y. Guo, 1988. The accumulation of hydrogen peroxide in senescing leaves and chloroplasts in relation to lipid peroxidation. *Acta Phytophysiologica Sin*., 1: 16–22

Lu, C.M. and A. Vonshak, 2002. Effects of Salinity stress on photosystem Ⅱ function in cyanobacterial Spirulina platensis cells. *Physiol. Plant*, 114: 405–413

Meenakumari, M., S.M. Thorsten, S.M. Laxa, D.M. Nunes, G.E. Florian, A.K. Stroher and D. Karl-Josef, 2009. Multiple redox and non-redox interactions define 2-Cys peroxiredoxin as a regulatory hub in the chloroplast. *Mol. Plant*, 2: 1273–1288

Nakano, Y. and K. Asada, 1987. Purification of ascorbate peroxidase in spinach chloroplasts; its inactivation in ascorbate-depleted medium and reactivation by monodehydroascorbate radical. *Plant Cell Physiol*., 28: 131–140

Nelson, N. and A. Ben-Shem, 2004. The complex architecture of oxygenic photosynthesis. *Nat. Rev. Mol. Cell Biol*., 5: 1–12

Nishiyama, Y., S.I. Allakhverdiev and N. Murata, 2011. Protein synthesis is the primary target of reactive oxygen species in the photoinhibition of photosystem Ⅱ. *Physiol. Plant*, 142: 35–46

Ohad, N. and J. Hirschberg, 1992. Mutations in the D1 subunit of photosystem Ⅱ distinguish between quinone and herbicide binding sites. *Plant Cell*, 4: 273–282

Pena-Ahumada, A., U. Kahmann, K.J. Dietz and M. Baier, 2006. Regulation of peroxiredoxin expression versus expression of Halliwell-Asada-Cycle enzymes during early seedling development of Arabidopsis thaliana. *Photosynth. Res*, 89: 99–112

Porebski, S., L.G. Bailey and B.R. Baum, 1997. Modification of a CTAB DNA extraction protocol for plants containing high polysaccharide and polyphenol components. *Plant Mol. Biol. Reporter*., 15: 8–15

Reddy, A.R., K.V. Chaitanya and M. Vivekanandan, 2004. Drought induced responses of photosynthesis and antioxidant metabolism in higher plants. *J. Plant Physiol*., 161: 1189–1202

Rhee, S.G. W. Jeong., T.S. Chang and H.A. Woo, 2007. Sulfiredoxin, the cysteine sulfinic acid reductase specific to 2-Cys peroxiredoxin: its discovery, mechanism of action, and biological significance. *Kidney Int.*, 72: S3–S8

Rouhier, N. and J.P. Jacquot, 2002. Plant peroxiredoxins: alternative hydroperoxide scavenging enzymes. *Photosynth. Res*., 74: 259–268

Santos, C.V.D. and P. Rey, 2006. Plant thioredoxins are key actors in the oxidative stress response. *Trends Plant Sci*., 11: 329–334

Shen, W.B., L.L. Xu, M.B. Ye and R.X. Zhang, 1996. Study on determination of ASP activity. *Plant Physiol. Commun*., 32: 203–205

Strasser, R.J. and A. Srivastava, 1995. Govindjee. Polyphasic chlorophyll a fluorescence transient in plants and cyanobacteria. *Photochem. Photobiol*., 61: 32–42

Sun, H.W., W.Q. Wang and Q.W. Meng, 2005. Functional mechanism and enzymatic and molecular characteristic of ascorbate peroxidase in plants. *Plant Physiol. Commun*., 41: 143–147

Sun, J., Y.X. Jia, S.R. Guo and J. Li, 2009. Effects of seawater stress on metabolism of reactive oxygen species and chlorophyll in chloroplasts of spinach (*Spinacia olerancea* L.). *Acta Ecol. Sin*., 29: 4361–4371

Vu, J.C.V., L.H. Allon and G. Gowes, 1987. Drought stress and elevated CO_2 effects on soybean ribulose biphosphate carboxylase activity and canopy photosynt hetic rates. *Plant Physiol*., 83: 573–579

Wang, J.Y., H. Ao and J. Zhang, 2003. *The Echnology and Experiment Principle of Plant Physiology*. Northeast Forestry University Press, Haerbin, China

Wei, G.Q., Z.J. Zhu, X.Z. Fang, J. Li and J. Cheng, 2004. The effects of NaCl stress on plant growth, chlorophyll fluorescence characteristics and active oxygen metabolism in seedlings of two cucumber cultivars. *Sci. Agric. Sin*., 37: 1754–1759

Winterbourn, C.C., 2008. Reconciling the chemistry and biology of reactive oxygen species. *Nat. Chem. Biol*., 4: 278–286

Wood, Z.A., L.B. Poole and P.A. Karohs, 2003. Peroxiredoxin evolution and the regulation of hydrogen peroxide signaling. *Science*, 300: 650–653

Xia, J., Y. Li and D. Zou, 2004. Effects of salinity stress on PSII in *Ulva lactuca* as probed by chlorophyll fluorescence measurements. *Aquat. Bot*., 80: 129–137

Yang, C.W., C.Y. Li, H.J. Yin, M. Ju and D.C. Shi, 2007. Physiological response of xiaobingmai (*Triticum aestivum-Agropyron intermedium*) to salt-stress and alkali-stress. *Acta Agron. Sin*., 8: 1255–1261

Ye, L.H., W.J. Shen, B.G. Zheng, T. Song, G.Q. Chen and C.G. Lv, 2013. Changes of photosynthetic membrane function and protein complexes in flag leaves of Liangyoupeijiu during leaf senescence. *Acta Agron. Sin*., 39: 2030–2038

Zhang, H.H., Q. Tian, G.J. Liu, Y.B. Hu, X.Y. Wu, Y. Tian and G.Y. Sun, 2013b. Responses of antioxidant enzyme and PSII electron transport in leaf of transgenic tobacco carrying *2-Cys Prx* to salt and light stresses. *Acta. Agron. Sin*., 39: 2023–2029

Zhang, H.H., X.L. Zhang, X. Li, J.N. Ding, W.X. Zhu, F. Qi, T. Zhang, Y. Tian and G.Y. Sun, 2012a. Effects of NaCl and Na_2CO_3 stresses on the growth and photosynthesis characteristics of *Morus alba* seedlings. *Chin. J. Appl. Ecol*., 23: 625–631

Zhang, H.H., X.L. Zhang, X. Li, N. Xu and G.Y. Sun, 2013a. Role of D1 protein turnover and xanthophylls cycle in protecting of photosystem II functions in leaves of *Morus alba* under NaCl stress. *Sci. Silvae Sin*., 49: 99–106

Zhang, Z., G. Li, H. Gao, T.L. Zhang, C. Yang, P. Liu and Q.W. Meng, 2012b. Characterization of photosynthetic performance during senescence in stay-green and quick-leaf-senescence *Zea mays* L. inbred lines. *Plos One*, 7: e42936

Zhu, H.J., R.G. Wang, S.L. Chen, Y.X. Zhang, N.Y. Li and J. Shao, 2007. Genotypic differences between *Populus euphratica* and *P. popularis* in antioxidative ability and salt tolerance under NaCl stress. *Acta Ecol. Sin*., 27: 4113–4121

(Received 04 January 2017; Accepted 21 March 2017)